Unipolar terahertz pulse formation in a nonequilibrium plasma channel formed by an ultrashort uv laser pulse

A. V. Bogatskaya,[1,2] E. A. Volkova,[3,*] and A. M. Popov[1,2]
[1]*Department of Physics, Moscow State University, 119991 Moscow, Russia*
[2]*P. N. Lebedev Physical Institute, RAS, Moscow, Russia*
[3]*D. V. Skobeltsyn Institute of Nuclear Physics, Moscow State University, Moscow, Russia*

(Received 28 December 2020; revised 12 May 2021; accepted 6 July 2021; published 4 August 2021)

We perform an alternative approach to produce highly unipolar terahertz pulses. The idea is based on the nonuniform amplification of seed ultrashort carrier-envelope phase (CEP) pulses in nonequilibrium fast relaxing plasma of air or nitrogen. If the gain coefficient drops significantly within the duration of a one-cycle CEP pulse, it undergoes significant distortion where the leading edge of the pulse is amplified and the trailing tail of opposite polarity is absorbed. The obtained results involve a self-consistent solution of the second-order wave equation and kinetic Boltzmann equation for the electron velocity distribution function relaxation.

DOI: 10.1103/PhysRevE.104.025202

I. INTRODUCTION

Continuous progress in the area of ultrafast nonlinear optics entails searching for new regimes of light-matter interaction. For example, producing single-cycle or subcycle extremely short pulses has engaged considerable interest due to their possibilities of real-time control of a number of intraatomic and intramolecular processes [1–5]. In this regard, special interest in unipolar pulses is motivated by their property to have a unidirectional action on charged particles, which opens up opportunities for their use to control the wave packet dynamics [6–8], including the qubit control [9] and accelerating of charged particles [10]. In particular, unipolar or subcycle terahertz pulses can be used for effective control of the Rydberg atom dynamics [11]. To date, strong subcycle, so-called quasi-unipolar, pulses containing a high-amplitude leading edge and a long decaying weak tail of opposite polarity can be generated in the optical, (mid) infrared [12–15] and terahertz frequency ranges [16–19]. There also exist a number of mechanisms to reach a higher degree of unipolarity, such as the soliton propagation of few-cycle ultrashort lasers in nonlinear asymmetric media [20–22] and irradiating a double foil target with intense few-cycle laser pulses [13,23].

In this work we devise an alternative approach for the generation of unipolar pulses with controllable characteristics in the terahertz frequency range, which we believe will make a contribution for further development of this area of research. The idea of the proposed method consists of partial distortion of an input ultrashort THz pulse during its amplification in photoionizing air plasma according to the mechanism proposed in [24]. Actually, the specific nature of electron velocity distribution function (EVDF) relaxation in nitrogen or air, which is mostly determined by the vibrational excitations of nitrogen molecules, reveals more rapid dynamics in comparison with atomic gases, such as xenon or krypton. As a consequence, the positive gain factor exists on times of an order or even less than single-cycle pulse duration, which gives rise to the formation of the unipolar pulse. In addition, if the level of amplification is high enough, the backward influence of the propagating THz pulse also should be taken into account [25].

The idea of using highly nonequilibrium plasma of a number of atomic and molecular gases to amplify low-frequency radiation was first proposed in [26,27] and then widely studied for the cases of both gas-discharge plasma sustained by the static electric field [28–31] and photoionized plasma [24,32,33]. It was shown that in the latter case the main requirement for the realization of this effect is the presence of a rather narrow multiphoton ionization peak in a gas with rapidly increasing energy dependence of a transport scattering cross section. To explain the idea of amplification in such a nonequilibrium plasma we will recall that the temporal evolution of the EVDF is usually governed by the diffusion-type kinetic equation in energy (or absolute velocity) space [34,35]. If the peak of photoelectrons is located in the energy interval with a growing transport cross section, the energy diffusion coefficient decreases with electron energy. As a result, fast diffusion of the low-energy part of photoelectrons causes shifting of their mean energy to the lower values even in the presence of a low intense electric field in plasma. It means that the electron component of plasma displaces opposite to the direction of the force of the electric field. Hence, the electrons are cooling while the electromagnetic wave is amplified. It should be noted here that this mechanism can be used specifically for the amplification of seed THz signals introduced into the plasma, but not for the independent signal generation. The best candidates for observing the amplification effect are rare gases such as xenon and krypton, since they are characterized by the Ramsauer minimum and, as a consequence, by an increasing transport cross section in the

*Corresponding author: annabogatskaya@gmail.com

energy range of several eV. The existence of an amplification effect in air or nitrogen plasma was also demonstrated in [36]. The necessary condition for an amplified pulse with the carrier frequency $\omega < \nu_{tr}$ ($[\nu_{tr} = N\sigma_{tr}(v)v$ is the transport frequency of electron-atom collisions in plasma, σ_{tr} is the transport collisional cross section, and N is the gas density] reads [26]

$$\frac{d}{dv}[v^2/\sigma_{tr}(v)] > 0, \tag{1}$$

which should be accomplished in the region of the photoionization peak. In air plasma the appropriate velocity range is about 7.5×10^7–1.0×10^8 cm/s (which corresponds to the energy range 1.5–2.0 eV) [36]. Such an initial position of the photoelectrons in air can be obtained through the three-photon ionization of an oxygen molecule (ionization potential 12.08 eV) irradiated by the third harmonic of a titanium-sapphire laser [37]. The presence of low vibrational states of the nitrogen molecule adds to rather fast relaxation of the electron energy spectrum in nitrogen (air). It was demonstrated [36] that for atmospheric pressure the possible duration of the THz pulse gain regime does not exceed ~20 ps, which allows one to amplify extremely short terahertz pulses. The key issue that accompanies the short amplification effect is the ability to generate intense unipolar pulses in the THz range. Specifically, if the gain coefficient drops significantly within the duration of the one-cycle carrier-envelope phase (CEP) pulse, that results in significant signal distortion where the leading half-period of the pulse is amplified and the trailing half-period is absorbed (or very slightly amplified). It is noteworthy that the proper consideration of this regime should be carried out by self-consistent solving the wave equation beyond the slowly varying amplitude approximation and kinetic Boltzmann equation for EVDF evolution in nonequiribrium plasma. Here we will also show that for rather high intensities of a propagating CEP pulse its backward influence on the EVDF evolution can additionally accelerate the formation of pulse unipolarity during the nonuniform amplification.

II. THE MODEL

Our modeling comprises the solution of the second-order wave equation for the ultrashort THz pulse propagation and amplification in the nonequilibrium plasma channel [25]:

$$\frac{\partial^2 \vec{E}(x,t)}{\partial x^2} = \frac{1}{c^2}\frac{\partial^2 \vec{E}(x,t)}{\partial t^2} + \frac{4\pi}{c^2}\frac{\partial \vec{j}(x,t)}{\partial t}. \tag{2}$$

Here $\vec{E}(x,t)$ is the vector of the electric field and $\vec{j}(x,t)$ is the density current response of the plasma channel. This response depends on the EVDF and is determined by the expression

$$\vec{j}(x,t) = -en_e \int \vec{v} f(x,\vec{v},t) d^3v, \tag{3}$$

where $f(x,\vec{v},t)$ is the EVDF, normalized according to the expression

$$\int f(x,\vec{v},t) d^3v = 1, \tag{4}$$

where n_e is the electron density. For rather high pressures the EVDF can be considered to be spatially local. Then it satisfies the Boltzmann equation [34,35] at each spatial point x of the plasma channel:

$$\frac{\partial f(x,\vec{v},t)}{\partial t} - \frac{e\vec{E}(x,t)}{m}\frac{\partial f}{\partial \vec{v}} = St(f), \tag{5}$$

where $St(f)$ is the collisional integral that takes into account both elastic and inelastic collisions of electrons.

If the electromagnetic wave is linearly polarized, the solution of Eq. (5) is typically represented as a series over the Legendre polynomials $P_n(\cos\vartheta)$:

$$f(x,\vec{v},t) = \sum_n f_n(x,v,t) P_n(\cos\vartheta). \tag{6}$$

Here f_n is the nth angle harmonic of the EVDF, and ϑ is the angle between the velocity and electric field strength vector (z-axis). Using decomposion (6) one can find that the current in plasma along the z-axis is determined only by the first angle harmonic:

$$j(x,t) = -\frac{4\pi e n_e}{3}\int v^3 f_1(x,v,t) dv, \tag{7}$$

while the zero-order harmonic stands for the distrubution of the electrons over the absolute value of velocity. If the anisotropy of the electron motion caused by the the external field in a plasma is weak, the so-called two-term decomposition for the EVDF can be applied where only two lowest harmonics in (6) are taken into account. In this case one obtains the set of equations for f_0 and f_1 harmonics at each spatial point of the pulse propagation:

$$\frac{\partial f_0(x,v,t)}{\partial t} = \frac{eE(x,t)}{3mv^2}\frac{\partial}{\partial v}[v^2 f_1(x,v,t)] + Q_0, \tag{8}$$

$$\frac{\partial f_1(x,v,t)}{\partial t} - \frac{eE(x,t)}{m}\frac{\partial f_0(x,v,t)}{\partial v} = Q_1. \tag{9}$$

Here $Q_0 = \frac{1}{4\pi}\int St(f) d\Omega$ and $Q_1 = \frac{3}{4\pi}\int \cos\vartheta St(f) d\Omega$ are collisional integrals for f_0 and f_1 respectively [34,35]. Direct calculations of the integrals for the elastic collisional terms $Q_0^{(el)}$ and $Q_1^{(el)}$ give rise to the following expressions [34]:

$$Q_0^{(el)} = -\frac{m}{M}\frac{1}{v^2}\frac{\partial}{\partial v}\left[\nu_{tr}(v)\left(v f_0 + \frac{T_g}{m}\frac{\partial f_0}{\partial v}\right)\right], \tag{10}$$

$$Q_1^{(el)} = -\nu_{tr}(v) f_1. \tag{11}$$

Here M is the mass of nitrogen molecule and T_g is the gas temperature. As for inelastic collisions, mainly vibrational excitation of the nitrogen molecules should be taken into account. The additional term [38]

$$Q_0^{(inel)} = -N\sum_i [\sigma_i^*(v) v f_0(x,v,t) + \sigma_i^*(V) V f_0(x,V,t)(V/v)] \tag{12}$$

should be added to the right part of Eq. (8). Here $\sigma_i^*(v)$ is the vibrational excitation cross section in the ith channel, and velocity V can be expressed through v via the relation

$$\frac{mV^2}{2} = \frac{mv^2}{2} + \varepsilon_i^{(v)}, \tag{13}$$

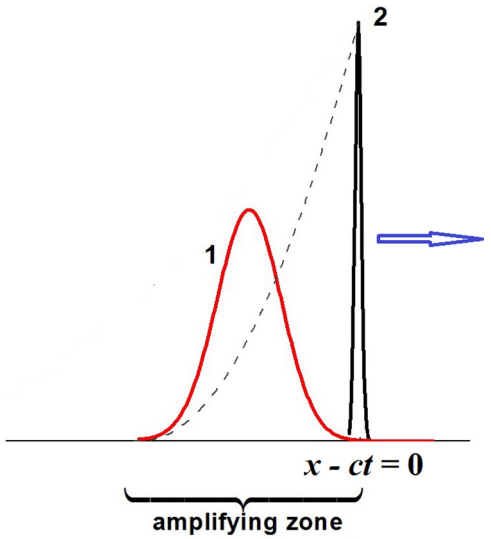

FIG. 1. General scheme of the unipolar THz pulse formation in the plasma channel formed by a femtosecond uv pulse. 1, seed THz pulse; 2, ionizing uv pulse. Arrow indicates the direction of pulse movement.

where $\varepsilon_i^{(v)}$ is the ith threshold of the N_2 molecule vibrational excitation. In our simulation eight lower excitation levels were considered. As the values of vibrational excitation cross sections for the oxygen molecule are significantly less in comparison with nitrogen ones, it is possible to neglect them at a qualitative level of study.

Below we use the same set of data for cross sections that was used in [36]. Here we also neglect the electron-electron collisional integral [34] as its effect on the EVDF evolution in air or nitrogen plasma at atmospheric pressure is rather small while considering electron concentrations up to $n_e = 10^{14}$ cm^{-3}.

The EVDF relaxation rate determines the spatial region where amplification of the ultrashort terahertz signal is possible. Thus, let us choose the initial conditions ($t = 0$) for Eq. (2) in the following way. The femtosecond pulse that forms nonequilibrium plasma channel is located at the point with coordinate $x = 0$, while the ultrashort THz pulse is introduced in unionized gas in the region of a negative x-coordinate. The sketch of the geometry in this study is presented in Fig. 1: the uv femtosecond and THz pulse follow one after another in the same direction, and at each instant of time the THz pulse is located in the nonuniform amplifying region formed by the uv pulse.

In this paper we do not discuss how the initial seed THz ultrashort pulse forms. It can be produced by the well-known mechanisms employing two-color laser pulses [39]. Typically, such generated THz pulses are rather short: up to one or two cycles of oscillations.

For further study we use the following procedure to introduce the initial THz pulse. First, it is more expedient to set the initial THz CEP pulse via the vector potential:

$$A[\xi \in (-\ell,\ 0)]|_{t=0} = A_0\left[\sin^5\left(\frac{\pi(\xi-\ell)}{\ell}\right)\sin\left(2\pi\frac{\xi-\ell}{\ell}\right)\right], \qquad (14)$$

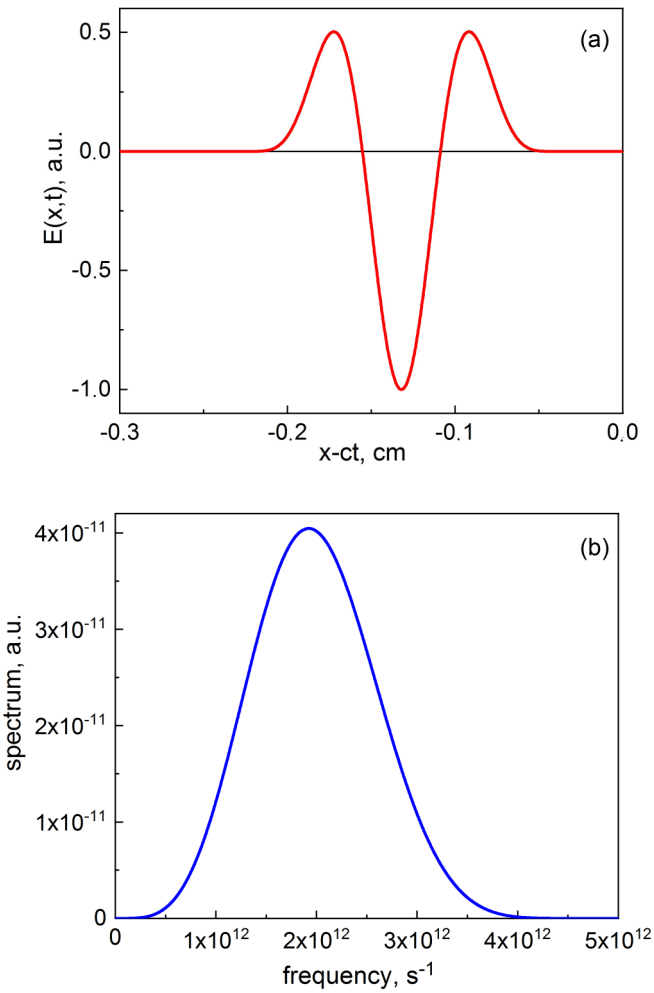

FIG. 2. Spatiotemporal (a) and spectral (b) characteristics of the initial CEP pulse normalized to unity.

where $\xi = x - ct$, and $\ell = 0.18$ cm is the spatial length of the pulse. Outside the given interval the vector potential is assumed to be zero. Then for the initial value of pulse electric field we get

$$E[x \in (-\ell,\ 0)]|_{t=0} = E_0 \times \left[\begin{array}{c}\sin^5\left(\frac{\pi(x-\ell)}{\ell}\right)\cos\left(2\pi\frac{x-\ell}{\ell}\right) \\ +\frac{5}{2}\sin^4\left(\frac{\pi(x-\ell)}{\ell}\right)\cos\left(\frac{\pi(x-\ell)}{\ell}\right)\sin\left(2\pi\frac{x-\ell}{\ell}\right)\end{array}\right], \qquad (15)$$

where $E_0 = \pi A_0/\ell$. Spatial-temporal and spectral characteristics of initial pulse are illustrated in Figs. 2(a) and 2(b). The pulse duration is about $\tau = \ell/c \approx 6$ ps, and its spectrum covers a wide frequency range from 0 to 4 THz with the central frequency near 2 THz. The given CEP pulse is characterized by the zero value of the integral $Q = \int E(x)dx$ taken over the pulse length. Such a pulse waveform is rather typical for those formed in modern experiments [40–42].

We assume that the ionizing femtosecond pulse propagates through the gas at the speed of light, creating a velocity-isotropic nonequilibrium distribution of photoelectrons behind it. Hence the initial condition for the anisotropic harmonic of the EVDF reads $f_1(x = ct, v) \equiv 0$. As about the

zero-order harmonic it was chosen in a form

$$f_0(x = ct, v) = \frac{1}{4\pi} \frac{m^{3/2}}{\Delta\varepsilon\sqrt{2\pi(mv^2/2)}} \exp\left[-\frac{(mv^2/2-\varepsilon_0)^2}{\Delta\varepsilon^2}\right]. \tag{16}$$

Such an expession corresponds to the Gaussian peak with central energy position ε_0 and energy width $\Delta\varepsilon$. If the ionization of oxygen molecules is governed by the third harmonic of the Ti-Sa laser, the photoelectron peak will have an energy of $\varepsilon_0 \approx 1.8$ eV. We also choose $\Delta\varepsilon = 0.1$ eV, which is typical for ionization by laser pulses of femtosecond duration. The above EVDF corresponds to the energy distribution of photoelectrons being considered in [36].

Wave equation (2) was solved jointly with the set of Boltzmann kinetic equations (8) and (9) at each spatial grid point since for rather strong amplified fields it is necessary to take into account the reconstruction of the EVDF caused by the propagating field. The general approach to the solution of the second-order wave equation (2) can be found in [25,38]. The total size of the spatial area for calculations was chosen to be $L = 1.0$ cm. The step of space discretization was $\Delta x = L/(2 \times 10^4) = 5 \times 10^{-5}$ cm. The temporal step of integration was $\Delta t = \Delta x/c \approx 1.67 \times 10^{-15}$ s. This step value allows to use the explicit scheme for the Boltzmann equation solution.

III. RESULTS AND DISCUSSION

In our simulations we consider different initial intensities of the propagating pulse. The initial peak electric field strength E_0 was expressed through the given intensity value as $E_0 = \sqrt{8\pi I_0/c}$. We assume the gas density N equal to 2.5×10^{19} cm^{-3} and the electron concentration in plasma to be $n_e = 3 \times 10^{13}$ cm^{-3}. The chosen value of electron density makes it possible to ignore the influence of electron-electron collisions in plasma that can result in a rather fast Maxwellization of EVFD [34] and destruction of the amplifying regime.

The typical spatial-temporal evolution of the signal amplified in the nonequilibrium nitrogen plasma channel of the length $L = 30$ cm is shown in Fig. 3. We note that due to dispersive spreading the pulse width increases approximately twice at the propagation length of 30 cm. It is also worth noting the following: since the gain is distributed strongly nonuniformly over the pulse length, only the front part of the pulse is significantly amplified, while the trailing edge is evenly absorbed. As a result, the amplified pulse with the nonzero value of the integral Q is formed during the propagation. The evolution of the pulse spectrum (see Fig. 4) clearly indicates the appearance of the static field component.

It must be stressed that the above results address the situation when the initial THz signal is strong enough and causes effective reconstruction of the EVDF. To compare the amplification of initially weak and high intense pulses we present data on the EVDF evolution at a spatial point 0.25 cm behind the leading edge of a uv laser pulse (Fig. 5). This spatial point corresponds to the trailing edge of the amplified pulse. In the case of low pulse intensity there is no backward influence on the EVDF, and all the EVDFs are the same at the given spatial point during the pulse propagation [Fig. 5(a)]. Another situation is observed for the initially intense THz pulse [Fig. 5(b)].

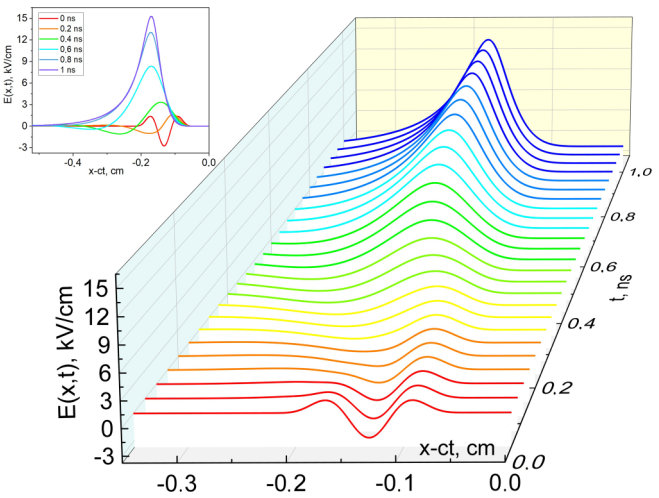

FIG. 3. Spatial-temporal evolution of the pulse [see expression (15)] propagating after the leading uv fs pulse (its position corresponds to the zero abscissa coordinate). Initial peak value of intensity is 10^4 W/cm^2.

In this case the energy from the plasma channel more effectively transforms to the THz signal energy, which provides rapid cooling of plasma electrons and diffuse spreading of EVDF. Such EVDF reconstruction by the propagating THz wavefield leads to the saturation of achievable gain.

To characterize the efficiency of transformation of the seed THz pulse to the unipolar one we introduce the degree of unipolarity in accordance with [7]

$$U = \frac{\int E(x)dx}{\int |E(x)|dx}, \tag{17}$$

where the integral is taken over all the pulse length during its propagation. The temporal evolution of the U-degree during the nonuniform pulse amplification for different values of the initial electric field strength corresponding to the peak intensities I_0 in the range from 0.01 W/cm^2 to 10^4 W/cm^2 is presented in Fig. 6.

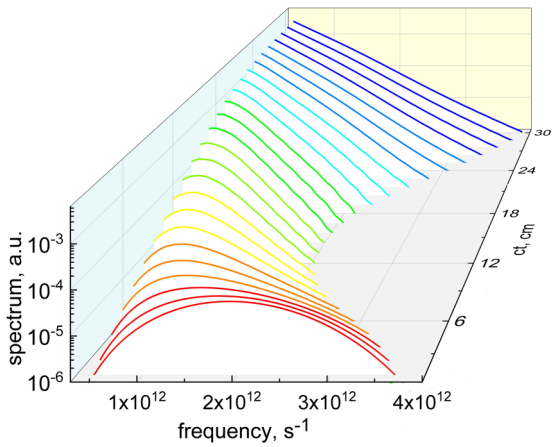

FIG. 4. The pulse spectrum and its evolution during the propagation and amplification in a nitrogen plasma channel.

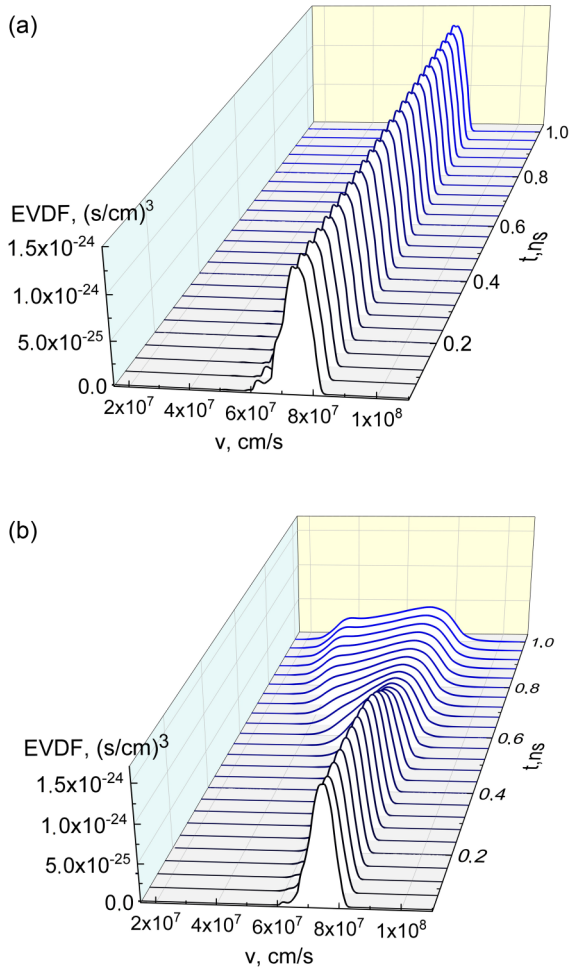

FIG. 5. Electron velocity distribution functions in dependence on propagation length in a spatial point behind the leading uv pulse of 0.25 cm for 0.01 W/cm^2 (a) and 10^4 W/cm^2 (b) initial peak THz pulse intensities.

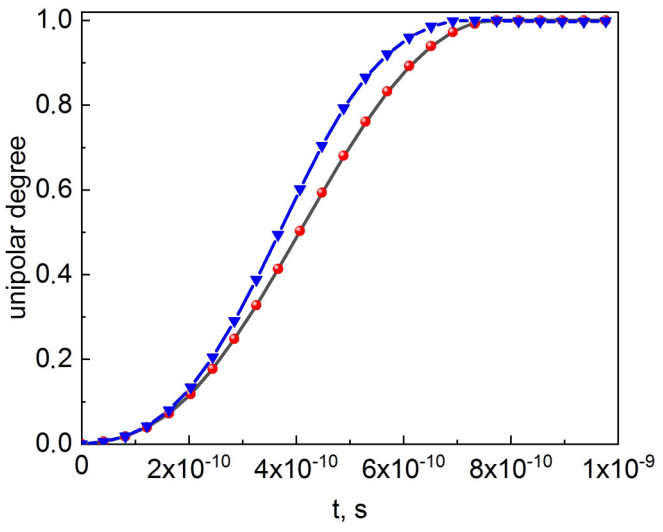

FIG. 6. The unipolarity degree of the THz pulse in dependence on propagation duration in a nonequilibrium nitrogen plasma channel for 0.01 (black solid line), 100 (red circles), and 10^4 W/cm^2 (blue line with triangles) initial peak pulse intensities.

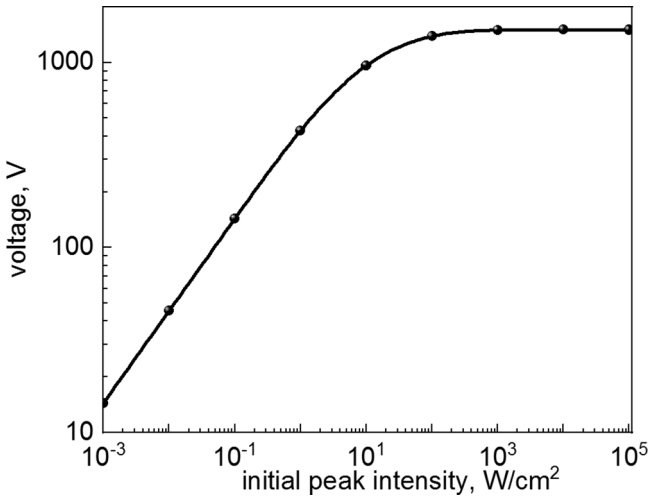

FIG. 7. The voltage carried by the unipolar pulse after its formation and amplification in a 30 cm nitrogen plasma channel in dependence on the initial pulse peak intensity.

The performed simulations demonstrate that the degree of unipolarity can reach the value up to unity for propagation times of ~0.7 ns (which is approximately 21 cm of plasma channel length) for any value of initial intensity within the considered range. Nevertheless, in the strong field limit when the backward influence of the THz field on the EVDF peak degradation is essential, the degree of unipolarity increases a bit rapidly.

To conclude the discussion, we have to show data for the voltage $V = \int E(x)dx$ accumulated in the forming unipolar pulse at the output of the 30 cm plasma channel depending on the initial peak intensity of the pulse (Fig. 7). For the given plasma channel parameters one can reach the voltage up to 1.5 kV for the initial peak intensity exceeding 100 W/cm^2. As has been mentioned before, the backward influence of the amplified wavefield on the EVDF for $I_0 \geqslant 100$ W/cm^2 leads to the EVFD peak spreading [see Fig. 5(b)] resulting in the voltage saturation. As the ultimate unipolar pulse length at the plasma channel output is about 0.15 cm one, can estimate its electric field strength as 10^4 V/cm.

For the pulse duration of several picoseconds this means that the electron will get the energy of several eV. That is enough for kick excitation and ionization of macromolecules and artificial atoms, quantum dots, and quantum wires in semiconductors, different types of impurities in solids, etc., which allows one to apply such unipolar pulses for the purposes of broadband THz spectroscopy.

Since the threshold of this regime is mainly determined by the relaxation rate of the nonequilibrium distribution function, preliminary analysis allows us to propose that due to the longer relaxation of EVDF in xenon plasma it will be possible to obtain unipolar THz pulses with higher energy. Another way to increase the energy conversion into the THz signal is to increase the electron concentration in plasma, but this will simultaneously lead to a faster Maxwellization of the EVDF. For the given parameters we are very close to the saturation of the gain effect.

IV. CONCLUSIONS

In summary, we propose a concept of obtaining intense unipolar THz pulses in photoionized air plasma channels. Based on the self-consisted modelling of ultrashort pulses propagation in fast-relaxing nonequilibrium air plasma of an extended channel we elicited the specific conditions of the proposed earlier gain regime when the pulse undergoes nonuniform amplification, which leads to the formation of intense THz pulses with a high degree of unipolarity. It was demonstrated that with the increase of pulse intensity its backward influence on the EVDF evolution brings to saturation the gain regime while it does not affect the achievement of signal unipolarity. Here it is also wise to compare the suggested method with the other existing mechanisms of producing highly intense ultrashort THz pulses. There is a continuous pursuit of increasing the efficiency of nonlinear-wave conversion in gases ionized by intense two-color laser radiation. In this regard the use of longer pumping wavelengths instead of the conventional Ti-Sa laser pulse and its second harmonic as well as application of other frequency ratios of two-color pumping fields and switching to the circular polarization has been extensively investigated [40–46], which enables us to reach the THz pulses with electric field amplitudes up to 1 GV/cm. Another trend is the production of subcycle duration pulses, which are characterized by the ultrabroadband spectrum for the purposes of THz spectroscopy [5,7,41]. The idea of the proposed method is to combine both mentioned trends, but its crucial advantage is not the extremely high signal intensity, but the ability to obtain unipolar pulses with a value of the U-factor close to unity, whereas in the most frequently cited papers the generated signals do not have this property. Such highly unipolar signals can have a strongly nonperturbative effect on various atomic-molecular systems in the "kick" regime, which will make it possible to propose alternative methods for objects' diagnostics in the terahertz range. Finally, we would briefly discuss the possibility of controlling the spectral characteristics of unipolar signals. We plan to optimize the phase of CEP seed pulse in order to obtain the unipolar pulse with maximum voltage. In addition, it was recently proposed [47] that applying a static magnetic field of tens of teslas along the pulse propagation in a nonequilibrium gas plasma allows one to manage the frequency bandwidth as well as the gain factor value in the terahertz range. So if one implements the proper nonuniformity of gain within the selected frequency range, prospectively this will allow us to produce intense unipolar THz pulses with tunable spectral characteristics.

ACKNOWLEDGMENTS

This work was supported by the RF President Grant No. MK-1932.2020.2 and the "Basis" Foundation (Grant No. 20-1-3-40-1).

[1] F. Krausz and M. Ivanov, Rev. Mod. Phys. **81**, 163 (2009).
[2] U. Keller, Appl. Phys. B **100**, 15 (2010).
[3] K. Ramasesha, S. R. Leone, and D. M. Neumark, Annu. Rev. Phys. Chem. **67**, 41 (2016).
[4] F. Calegari, G. Sansone, S. Stagira, C. Vozzi, and M. Nisoli, J. Phys. B **49**, 062001 (2016).
[5] X. Chai, X. Ropagnol, S. M. Raeis-Zadeh, M. Reid, S. Safavi-Naeini, and T. Ozaki, Phys. Rev. Lett. **121**, 143901 (2018).
[6] R. Arkhipov, A. V. Pakhomov, M. V. Arkhipov, A. Demircan, U. Morgner, N. N. Rosanov, and I. Babushkin, Opt. Express **28**, 17020 (2020).
[7] R. M. Arkhipov, A. V. Pakhomov, M. V. Arkhipov, A. Demircan, U. Morgner, N. N. Rosanov, and I. Babushkin, Phys. Rev. A **101**, 043838 (2020).
[8] X. Zhang and R. R. Jones, New J. Phys. **11**, 105050 (2009).
[9] M. V. Bastrakova, N. V. Klenovand, and A. M. Satanin, JETP **131**, 507 (2020).
[10] B.-S. Xie, M.-P. Liu, and N.-Y. Wang, Appl. Phys. Lett. **91**, 011118 (2007).
[11] A. Wetzels, A. Gürtler, L. D. Noordam, F. Robicheaux, C. Dinu, H. G. Muller, M. J. J. Vrakking, and W. J. van der Zande, Phys. Rev. Lett. **89**, 273003 (2002).
[12] M. T. Hassan, T. T. Luu, A. Moulet, O. Raskazovskaya, P. Zhokhov, M. Garg, N. Karpowicz, A. M. Zheltikov, V. Pervak, F. Krausz, and E. Goulielmakis, Nature (London) **530**, 66 (2016).
[13] H.-C. Wu and J. Meyer-ter-Vehn, Nat. Photonics **6**, 304 (2012).
[14] J. Xu, B. Shen, X. Zhang, Y. Shi, L. Ji, L. Zhang, T. Xu, W. Wang, X. Zhao, and Z. Xu, Sci. Rep. **8**, 2669 (2018).
[15] W.-H. Huang, Y. Zhao, S. Kusama, F. Kumaki, C.-W. Luo, and T. Fuji, Opt. Express **28**, 36527 (2020).
[16] K. Reimann, Rep. Prog. Phys. **70**, 1597 (2007).
[17] H. G. Roskos, M. D. Thomson, M. Kreβ, and T. Löffler, Laser Photonics Rev. **1**, 349 (2007).
[18] Y. Gao, T. Drake, Z. Chen, and M. F. DeCamp, Opt. Lett. **33**, 2776 (2008).
[19] M. I. Bakunov, A. V. Maslov, and M. V. Tsarev, Phys. Rev. A **95**, 063817 (2017).
[20] V. P. Kalosha and J. Herrmann, Phys. Rev. Lett. **83**, 544 (1999).
[21] X. Song, W. Yang, Z. Zeng, R. Li, and Z. Xu, Phys. Rev. A **82**, 053821 (2010).
[22] N. V. Vysotina, N. N. Rosanov, and V. E. Semenov, Opt. Spectrosc. **106**, 713 (2009).
[23] W. J. Ma, J. H. Bin, H. Y. Wang, M. Yeung, C. Kreuzer, M. Streeter, P.S. Foster, S. Cousens, D. Kiefer, B. Dromey, X.Q. Yan, J. Meyer-ter-Vehn, M. Zepf, and J. Schreiber, Phys. Rev. Lett. **113**, 235002 (2014).
[24] A. V. Bogatskaya and A. M. Popov, JETP Lett. **97**, 388 (2013).
[25] A. V. Bogatskaya, E. A. Volkova, and A. M. Popov, Laser Phys. **29**, 086002 (2019).
[26] G. Bekefi, J. L. Hirshfield, and S. C. Brown, Phys. Fluids **4**, 173 (1961).
[27] F. V. Bunkin, A. E. Kazakov, and M. V. Fedorov, Sov. Phys. Usp. **15**, 416 (1973).
[28] N. L. Aleksandrov and A. P. Napartovich, Phys. Usp. **36**, 107 (1993).
[29] N. A. Dyatko, A. P. Napartovich, S. Sakadzic, Z. Petrovic, and Z. Raspopovic, J. Phys. D **33**, 375 (2000).

[30] A. V. Bogatskaya and A. M. Popov, J. Phys. D **49**, 025203 (2016).
[31] C. Yuan, J. Yao, E. A. Bogdanov, A. A. Kudryavtsev, and Z. Zhou, Phys. Rev. E **101**, 031202(R) (2020).
[32] A. V. Bogatskaya, I. V. Smetanin, E. A. Volkova, and A. M. Popov, Laser Part. Beams **33**, 17 (2015).
[33] A. V. Bogatskaya, N. E. Gnezdovskaia, E. A. Volkova, and A. M. Popov, Plasma Sources Sci. Technol. **29**, 105016 (2020).
[34] V. L. Ginzburg and A. V. Gurevich, Sov. Phys. Usp. **3**, 115 (1960).
[35] Y. u. P. Raizer, *Laser-Induced Discharge Phenomena* (Consultants Bureau, New York, 1974).
[36] A. V. Bogatskaya, E. A. Volkova, and A. M. Popov, J. Phys. D **47**, 185202 (2014).
[37] V. D. Zvorykin, S. A. Goncharov, A. A. Ionin, D. V. Mokrousova, S. V. Ryabchuk, L. V. Seleznev, E. S. Sunchugasheva, N. N. Ustinovskii, and A V Shutov, Quant. Electron. **47**, 319 (2017).
[38] A. V. Bogatskaya, E. A. Volkova, and A. M. Popov, J. Exp. Theor. Phys. **130**, 649 (2020).
[39] K. Y. Kim, J. H. Glownia, A. J. Taylor, and G. Rodriguez, Opt. Express **15**, 4577 (2007).
[40] T. I. Oh, Y. S. You, N. Jhajj, E. W. Rosenthal, H. M. Milchberg, and K. Y. Kim, New J. Phys. **15**, 075002 (2013).
[41] T. Seifert, S. Jaiswal, M. Sajadi, G. Jakob, S. Winnerl, M. Wolf, M. Kläui, and T. Kampfrath, Appl. Phys. Lett. **110**, 252402 (2017).
[42] T. Balčiūnas, D. Lorenc, M. Ivanov, O. Smirnova, A. M. Zheltikov, D. Dietze, K. Unterrainer, T. Rathje, G. G. Paulus, A. Baltuška, and S. Haessler, Opt. Express **23**, 15278 (2015).
[43] V. A. Tulsky, M. Baghery, U. Saalmann, and S. V. Popruzhenko, Phys. Rev. A **98**, 053415 (2018).
[44] V. Yu. Fedorov and S. Tzortzakis, Phys. Rev. A **97**, 063842 (2018).
[45] A. Nguyen, P. González de Alaiza Martínez, I. Thiele, S. Skupin and L. Bergé, New J. Phys. **20**, 033026 (2018).
[46] C. Meng, W. Chen, X. Wang, Zh. Lü, Y. Huang, J. Liu, D. Zhang, Z. Zhao, and J. Yuan, Appl. Phys. Lett. **109**, 131105 (2016).
[47] A. V. Bogatskaya, N. E. Gnezdovskaia, and A. M. Popov, Phys. Rev. E **102**, 043202 (2020).